Temporal relaxation of nonequilibrium in Y-Ba-Cu-O measured from transient photoimpedance response

N. Bluzer
Westinghouse Advanced Technology Division, Baltimore, Maryland 21203
(Received 26 February 1991; revised manuscript received 28 June 1991)

Nonequilibrium in Y-Ba-Cu-O thin films biased with a dc current is photoinduced by exposure to 300-fsec 2-eV laser pulses. The photoinduced nonequilibrium transients were measured in the superconducting, transition, and normal states occurring between 7 and 200 K. The photoabsorption produced temporal changes in the sample's impedance, which manifest themselves as transient voltage signals occurring across the samples during the nonequilibrium's relaxation process. At and above T_c, the observed photoresponse is thermal. Below T_c, a quantum response is obtained corresponding to changes in the Cooper-pair populations. In the zero-resistance superconducting state, a positive signal corresponds to quasiparticle generation and a negative signal corresponds to quasiparticle recombination.

I. INTRODUCTION

Nonequilibrium properties of superconductors are a very important area of study. Inherently the nonequilibrium properties of superconductors provide (a) fundamental insight into the mechanism of superconductivity and (b) information needed for the application of these materials. Hence, it is not surprising that so much attention has been focused in this area.[1-4] In this paper we present transient photoresponse measurements on Y-Ba-Cu-O between 7 and 200 K. The data are analyzed in terms of the thermalization process of electrons, quasiparticles and phonons. Good agreement is obtained between measurements and calculations. Before presenting details on this experiment we briefly review conventional techniques for studying nonequilibrium in superconductors.

Often these different techniques produce and measure different forms of deviation from the superconductors thermal equilibrium state. Electrical injection has been used to produce and study the branch imbalance lifetime (τ_Q) between holelike and electronlike quasiparticles. The branch imbalance lifetime is obtained from the changes in the I-V characteristics[5] of a double superconductor (S) insulator (I) tunnel junction structure ($S/I/S/I/S$). The branch imbalance lifetime has also been measured from chemical potential differences between the condensate and the quasiparticles[6] on structures with normal (N) and superconductive (S) electrodes connected to a double tunnel junction structure ($S/I/S/I/N$). A variation on the chemical potential method made use of quasiparticle diffusion to obtain the lifetime τ_Q from the chemical potential decay length[7] differences between the condensate and the quasiparticles.

These measurements[5-7] required complicated sample geometries and a recombination[6,7] lifetime (τ_R) larger than the branch imbalance lifetime (τ_Q). Simplification of the sample geometry was achieved by using chopped dc with a small continuous rf currents to measure, near T_c, kinetic inductance[8] changes from which the recombination lifetime[9] τ_R is determined. Unfortunately these measurements, made on tin, were limited to a regime near T_c ($0.95 < T/T_c \leq 0.995$), where changes in the kinetic inductance are significant with temperature and bias current. Testardi[10] further simplified formation of nonequilibrium by using photodepairing, thereby dispensing with the need for complicated quasiparticle generation structures. Making use of such simplifications, we report on measurements made on Y-Ba-Cu-O using a different method.

II. EXPERIMENTAL APPROACH

The photoresponse of Y-Ba-Cu-O was measured with a transient photoimpedence response (TPR) technique[11] that combines some elements of previous experiments[9,10-13] to synthesize a simplified approach for measuring nonequilibrium properties. Simple unpatterned thin-film samples are used with the TPR method, thereby dispensing with technologically demanding stacked tunnel junctions[5,6] structures and/or special contact electrodes.[7] The samples are configured into a Corbino geometry simply by shadow evaporating two concentric gold contacts, illustrated in Fig. 1. The contact's geometry corresponds to the cross section of a microcoax

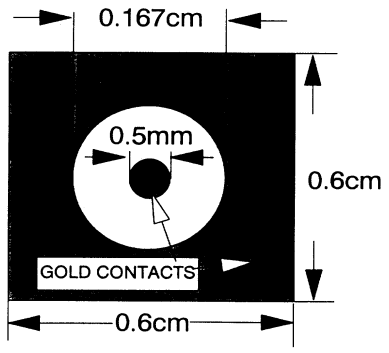

FIG. 1. Corbino disk sample geometry for minimization of fluxoids formation.

to which the sample is electrically connected by pressure (see Fig. 2). For a Corbino geometry the bias current does not produce a magnetic field that crosses the sample's plane. Accordingly, formation of fluxons is minimized. The (0.212-cm-diam) microcoax is thermally and mechanically attached to the cryostat's cold finger. Two silicon diode temperature sensors are used to monitor and maintain the sample's temperature within 0.1 K. The short microcoax (≈ 5 cm) minimizes frequency dispersion effects. A Wiltron bias "T" ac couples (100 MHz to 65 GHz) the sample's output signal to the 70-GHz Hypres oscilloscope and provides a low-frequency port to bias the sample with a dc current I_0.

TPR signals, $e_{\rm osc}(t)$, were produced when the samples, biased with a dc current I_0, were illuminated through the substrate with 620-nm 300-fsec 2-kHz laser pulses with an energy between 0.1 and 3 μJ per pulse and a spot size ≈ 0.22 cm (see Fig. 2). Temporal transients in the sample's impedance, caused by photoabsorption, varied according to the sample's experimental condition and the experiment's transfer function. The experiment's transfer function is considered next.

In the superconducting state, the samples can be either in the (1) zero resistance state or (2) resistive state. In the resistive state, the sample is represented by a changing photoresistance $r(t)$ in series with a magnetic inductance (L_G) and a contact resistance R [see Fig. 3(a)]. In the zero resistance superconductivity state the sample is represented as a changing kinetic inductance[8,11,12,14,15] [photoinductance $\eta(t)$] in series with a magnetic inductance ($L_G \approx 30$ pH) and a resistance (R) [see Fig. 3(b)]. The normal channel, per the London two-fluid model,[14] acts as a shunting resistance across the kinetic inductance [Fig. 3(b)], which is the ac signal generator in this experiment. The normal channel qualitatively does not affect output signal $E_{\rm osc}(t)$, however, it does attenuate its amplitude.[11] Accordingly, without the loss of any qualitative information, attenuations of the output signal by the normal channel have been neglected.[11]

The oscilloscope's output signal $e_{\rm osc}(t)$, is related to the changes in the kinetic inductance by[11]

$$\frac{d[I_0\eta(t)]}{dt} \cong \frac{L_G}{50}\frac{de_{\rm osc}(t)}{dt} + e_{\rm osc}(t) + \frac{1}{50C}\int_0^t e_{\rm osc}(t')dt'. \quad (1)$$

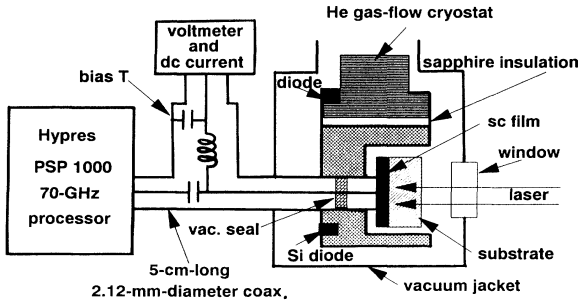

FIG. 2. Experimental setup.

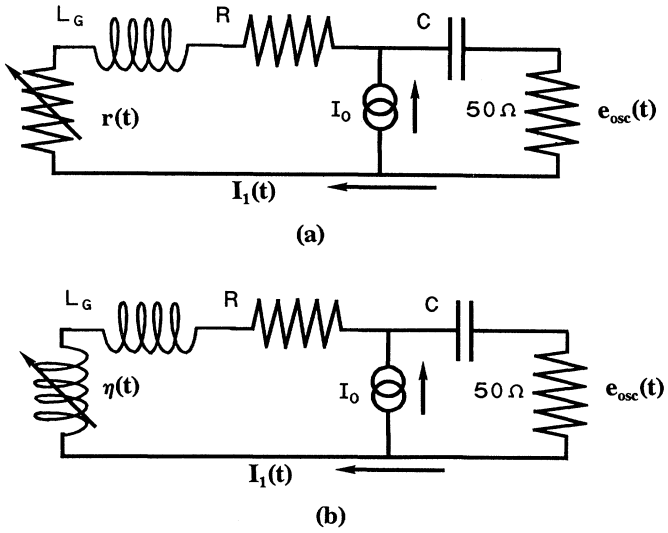

FIG. 3. Equivalent circuit for superconducting state (bottom) and resistive state (top). The capacitor $C = 300$ pF represents the bias T coupling capacitance between the sample and the oscilloscope represented here as the 50-Ω load.

The contact resistance R is neglected, since it is much less than the microcoax's and scope's 50-Ω impedances. The three terms on the right in Eq. (1) correspond, respectively, to the potential drops across; the inductance L_G, the 50-Ω impedance, and the coupling capacitor C (≈ 300 pF) between the scope and the sample. Similarly, for changes in the sample's resistance $r(t)$ the output signal $e_{\rm osc}(t)$ can be expressed as;[11]

$$I_0 r(t) \cong e_{\rm osc}(t) + \frac{L_G}{50}\frac{de_{\rm osc}(t)}{dt} + \frac{1}{50C}\int_0^t e_{\rm osc}(t')dt'. \quad (2)$$

Where the ac voltage signal caused by the changing resistor $r(t)$ is equal to the voltage drops developed across the microcoax's 50-Ω impedance, the inductor ($L_G \cong 30$ pH) and the coupling capacitor ($C \cong 300$ pF). These transfer functions, Eqs. (1) and (2), are used in the data analysis.

III. EXPERIMENTAL RESULTS

The experimental data on smooth Y-Ba-Cu-O thin films were recorded between 7 and 200 K for the normal, transition, and superconductivity states. The characteristics of the samples studied are given in Table I. Sample films Nos. 1 and 2 were made at Westinghouse, and sample films Nos. 3 and 4 were made at Stanford. The samples had approximately the same resistive temperature coefficient (1 $\mu\Omega$ cm/K). The resistivity at T_c for the films prepared by sputtering was about 80 $\mu\Omega$ cm, while the laser ablated film exhibited a higher resistivity ~ 140 $\mu\Omega$ cm. Over 200 photoresponse traces were measured on Y-Ba-Cu-O and were recorded at different temperatures, dc bias currents (10–300 mA) and laser fluences (0.1–2.4 μJ). Care was used to maintain the laser beam focused on the sample. However, maintaining

TABLE I. Characteristics of Y-Ba-Cu-O films used in this study. All films have a c-axis orientation.

Sample No.	Thickness (nm)	J_c (A/cm^2)	T_c (K)	ΔT_c (K)	$\rho(T_c)$ ($\mu\Omega$ cm)	$\Delta\rho/\Delta T$ ($T > T_c$) ($\mu\Omega$ cm/K)	$\Delta\rho(T_c)/\Delta T$ ($\mu\Omega$ cm/K	Deposition method	Substrate material
1	20	5×10^6 at 77 K	86.8	2	75	1	37	Sputtered	$LaAlO_3$
2	80	5×10^6 at 77 K	85	3	90	1	30	Sputtered	MgO
3	50	10^7 at 4.2 K	85	1.5	70	1	47	Sputtered	MgO
4	30	2×10^7 at 4.2 K	87	1.5	140	1.1	93	Laser ablation	$LaAlO_3$

optimal focus was difficult because of the complicated setup and thermal expansion and contraction of the cryostat. To minimize defocusing problems we periodically realigned the sample with the laser beam. For the dc bias currents used, the observed photoresponse was linear and the preponderance of data reported on is for bias currents between 10 and 50 mA. The output voltage signal measured on the oscilloscope is presented here in a normalized form as an impedance trace obtained by dividing the output voltage signal $e_{osc}(t)$ by the dc bias current I_0.

The normal-state experimental results, on a representative group of three films (Nos. 1, 2, and 3), are given in Tables II and III. Typically, the signal exhibits a sharp rise time (<50 psec) followed by a slower decay (see Fig. 4). The photoresponse is characterized by the peak amplitude value and the decay time constant. Between T_c and 200 K, all the samples studied exhibited a decreasing photoresponse amplitude with increasing temperature. A typical decrease in the photoresponse amplitude with increasing temperature is given in Fig. 5 for sample No. 2. The maximum photoresponse, corresponding to the maximum change in the sample's impedance, occurs immediately following the absorption of the laser pulse's energy. The time constant for the decaying portion of $e_{osc}(t)$ in the normal state shows almost no temperature dependence. It appears that the relaxation-time constant increases with film thickness (see Table II).

Typically, the photoresponsivity at T_c (see Table IV) is at least ten times larger than the normal-state photoresponsivity. Also, the relaxation-time constant at T_c is significantly larger than the relaxation time constant in the normal state (see plot in Fig. 6). Below T_c, the photoresponse relaxation-time constant for the positive signal is smaller than the time constant for either the normal or transition states.

Below T_c, the photoimpedance response measured on four films (see Table II) was characterized by photoresponse amplitude, relaxation slope and shape. Typically, the photoimpedance transient response started with a fast positive rise time (<50 psec) followed by a slower decaying signal. The decaying portion of the transient photoimpedance response (TPR) signal is grouped into three categories. The most conventional TPR signal below T_c is qualitatively similar to the trace illustrated in Fig. 4 except the signal's decay portion, for some traces, cannot be described by an exponential with a single relaxation-time constant as evident from the semilog plot (see Fig. 7). A second very important category of TPR signals are a positive signal followed by a negative photoimpedance response signal (see Fig. 8). A third category of TPR signals exhibits a nonmonotonic positive response signal with a negative photoresponse amplitude for the final portion of the relaxation process (see Fig. 9).

It is difficult to assign a single relaxation-time constant to these complicated TPR signals. We have characterized the decay of the positive portion of the TPR signal by at most two time constants. Between 7 and 85 K the decay time constant of the TPR signal's positive ampli-

TABLE II. Photoresponse of Y-Ba-Cu-O films exposed to 2-eV 300-psec laser pulses. Photoresponse in the resistive state was normalized by the film's resistance, whereas photoresponse in the zero dc resistance superconducting state was normalized by the film's kinetic inductance. The values of the kinetic inductance listed are the calculated theoretical values.

Sample No.	Responsivity ($1/\mu$J) $T\simeq100$ K	$T\cong200$ K	T_c	$T\leq60$ K	$T\approx80$ K	Relaxation (nsec) $100<T<200$	T_c	$10<T<60$ K	$T\approx80$ K	Kinetic inductance at 4.2 K (L^0_{KI})
1	0.0135	0.002	0.076	0.2	4.18	0.7	1.8	0.15	0.6	257 fH
2	0.008	0.001	0.43	0.14	0.01	2.5	4.5	0.3	1.0	63 fH
3	0.0188	0.005	0.308	0.35	0.84	2.5	6.2		0.80	102 fH
4			1.12	0.66	0.72		0.66	0.28	0.6	342 fH

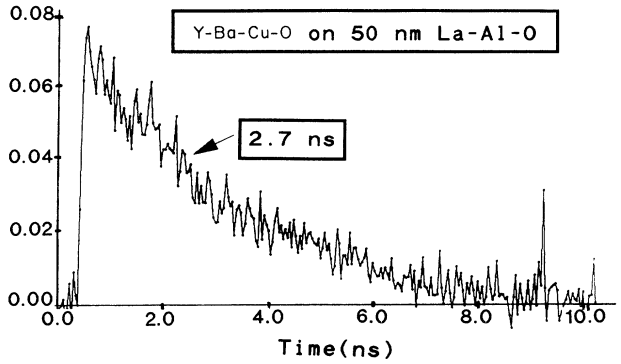

FIG. 4. Transient photoresponse of Y-Ba-Cu-O in normal state at 165 K with a 20-mA bias and exposed to 1.94 μJ of laser fluence. The ordinate (in units of Ω) corresponds to the measured transient voltage signal divided by the dc bias current.

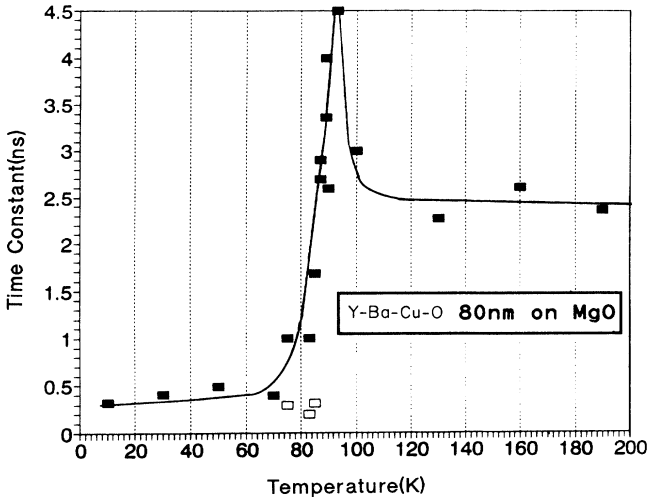

FIG. 6. Relaxation-time constant of Y-Ba-Cu-O vs temperature. The curve was drown only as a guide. Closer to T_c the photoresponse relaxation-time constant cannot be represented by a single value; hence, both open and filled rectangles were included in this figure.

tude increases from about 200 to about 800 psec (see Table II and Fig. 6). The trailing part of the TPR signal exhibits a time constant typically greater than 5 nsec.

The amplitude of the TPR signal below T_c is typically linear with bias current and becomes temperature dependent only when we approach T_c. Near T_c the TPR signal amplitude rapidly increases as is evident from Table V for a 20-nm-thick Y-Ba-Cu-O film on LaAlO. Similar increases are observed for the other Y-Ba-Cu-O films examined and the results are tabulated in Table II. Interpretation of the experimental data follows.

IV. DATA INTERPRETATION

Interpretation of the photoresponse for each state is consistent with and facilitated by the results obtained from the other two states. Clearly a proper interpretation requires a self-consistent explanation of the data in the normal, transition and superconducting states. Given the complexity of interpreting the photoresponse data, we will start first by interpreting the simplest photoresponse and that occurs in the normal state.

A. Normal-state photoresponse

It will be shown that the TPR signal's amplitude and decay time constant in the normal state are consistent with a thermal response. The transient photoresponse signal (see Fig. 4) is modeled as a thermally induced time-dependent resistance [Fig. 3(a)], starting with a steep positive rise (<50 psec) followed by a gradual decay.

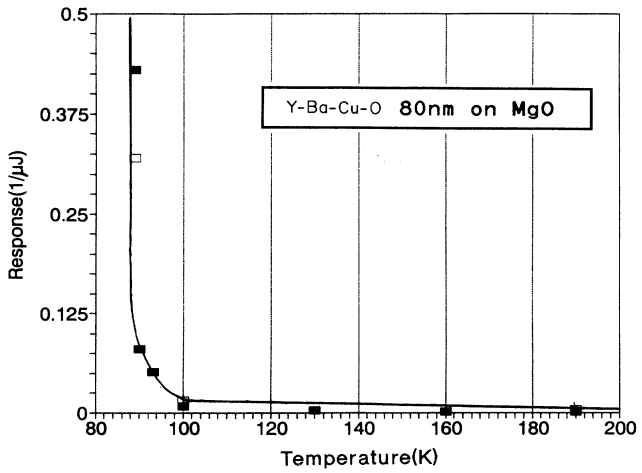

FIG. 5. Normalized measured photoresponse amplitude (filled squares) of Y-Ba-Cu-O thin film in the transition and normal states. The open squares and the plotted curve represents the calculated response.

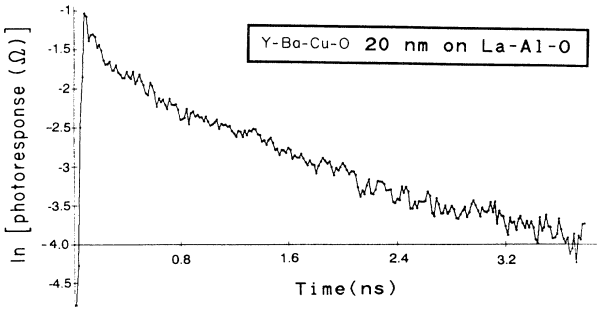

FIG. 7. Semilog plot of the photoimpedance response for Y-Ba-Cu-O exposed to 0.29 μJ laser fluence at 83 K and biased with 29.6 mA exhibiting a decay that cannot be represented by a single time constant.

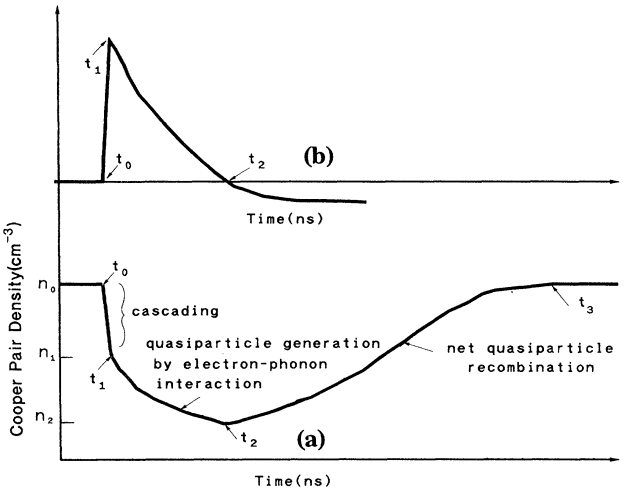

FIG. 8. (a) The Cooper-pair density plotted as a function of time. At time t_0 the laser pulse is absorbed, and the Cooper-pair density is reduced quickly from n_0 to n_1 by electron-electron interaction. At time t_1 electron-phonon processes start to dominate, and quasiparticles continue to be generated at a slower rate. Finally, at time t_2, enough phonons have escaped into the substrate to provide conditions favorable for quasiparticle recombination. At time t_3 the transient nonequilibrium conditions have dissipated and the Cooper-pair density again becomes n_0. Since the signal is proportional to the derivative of the kinetic inductance ($\eta \propto 1/n$) it should be evident that the derivative of curve a correspond to the measured signals illustrated by curve (b).

The steep positive rise and its amplitude correspond to the maximum resistance increase occurring immediately following photoabsorption. The thermal response amplitude $\mathcal{R}(T)$ of Y-Ba-Cu-O films normalized by the laser's fluence, is expressed in terms of film's resistivity $[\rho(T)]$, resistivity's temperature coefficient $[\Delta\rho(T)/\Delta T]$, the incident laser power $[L(\mu J)]$, and the change in the films temperature (ΔT), as

$$\mathcal{R}(T)=\frac{\Delta\rho(T)}{\Delta T}\frac{1}{\rho(T)}\frac{\Delta T}{L(\mu J)} . \tag{3}$$

The film's temperature rise ΔT is computed from the specific heat[16] $C(T)$, the sample thickness d, the optical absorption coefficient[17] $\alpha \cong 65$ nm for 2-eV photons, the laser beam's diameter cross section $A_L \approx 0.038$ cm^2, the sample's cross section $A_S \approx 0.022$ cm^2, and the optical transmission $T_{op} \approx 0.5$ through the window and film's substrate as

$$\Delta T=\frac{L(\mu J)}{A_L}\frac{T_{op}}{dC(T)}[1-\exp(-\alpha d)] . \tag{4}$$

Combining Eqs. (3) and (4), we obtain an expression for the normalized thermal photoresponse amplitude;

$$\mathcal{R}(T)=\frac{26.3}{\rho(T)}\frac{1-\exp(-\alpha d)}{C(T)}\frac{T_{op}}{d}\frac{\Delta\rho(T)}{\Delta T} . \tag{5}$$

The temperature dependence of the Y-Ba-Cu-O film resistivities has been measured with the relevant parameters and is given in Table I. The calculated and measured photoresponsivities for three films are given in Table III below. Agreement between the experimental data and calculations is typically within a factor of 2 with the worst case being within a factor of 4. The differences are

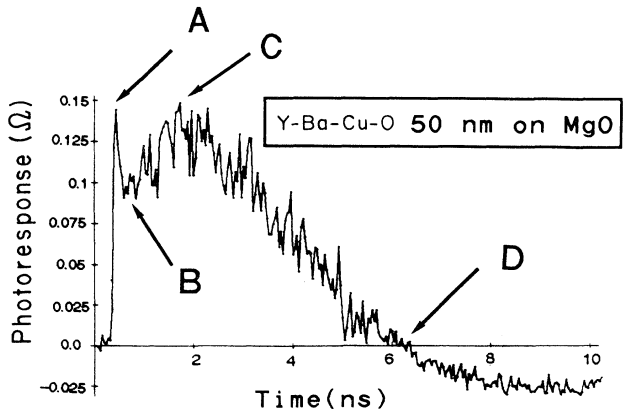

FIG. 9. Photoimpedance response of Y-Ba-Cu-O at 75 K biased with 20.9 mA and exposed to a 1.99-μJ laser fluence exhibiting a nonmonotonical positive response signal and a negative signal. A change in state from a zero-resistance superconducting state to a resistive state occurs at point B.

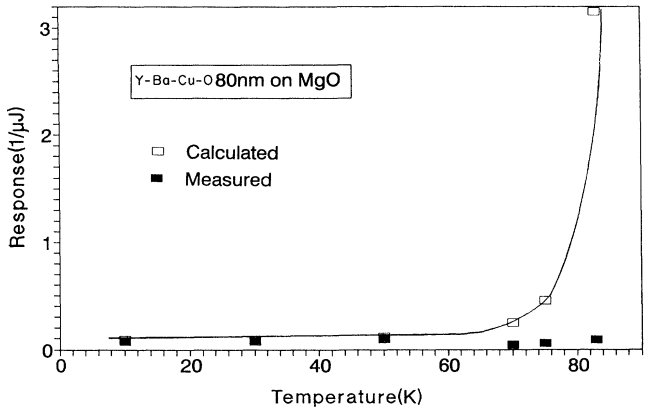

FIG. 10. Photoresponse of Y-Ba-Cu-O due to kinetic inductance changes. The photoresponse has been normalized in Table V by using Eq. (10). The drawn curve represents the calculated photoresponse.

TABLE III. Measured and calculated photoresponse amplitude for Y-Ba-Cu-O thin films at 100 and 200 K.

	Measured $(1/\mu J)$		Calculated $(1/\mu J)$	
Film No.	$R(100)$	$R(200)$	$R(100)$	$R(200)$
1	0.0135	0.002	0.013	0.0038
2	0.0084	0.001	0.015	0.0038
3	0.0188	0.005	0.027	0.0076

attributed to the uncertainty in the amount of laser energy absorbed, by the samples, and focus problems. Such an agreement between experiment and calculations, over a wide temperature range, gives support to the assertion that the normal-state photoresponse amplitude is thermal.

Next we examine if the photoresponse rise and relaxation times are consistent with a thermal photoresponse. The fast rise time corresponds to the energy photodeposition process in Y-Ba-Cu-O films, while the slower relaxation process corresponds to the removal of the photodeposited energy by phonon emission from the Y-Ba-Cu-O film into the substrate.

Initially, the 300-fsec laser pulse photoexcites normal electrons to about 2 eV above the Y-Ba-Cu-O Fermi surface. Thermalization of the photoexcited electrons occurs via electron-electron and electron-phonon interactions. The duration and the type of interactions occurring during the thermalization process depends on the time constants of the electron-electron (τ_{ee}) and electron-phonon ($\tau_{e\text{-ph}}$) interactions.[18] Equations for τ_{ee} and $\tau_{e\text{-ph}}$ (Ref. 19) in terms of the Fermi energy (E_F), the excess electron's energy (ε), and the phonon frequency (ω) are

$$\tau_{ee}=\left[\frac{\kappa}{p_F}+\frac{16}{\pi}\frac{q_D}{p_F}(\beta^2+\beta)\right]^{-1}\frac{64}{\pi^4}\frac{h}{e}\frac{E_F(\text{eV})}{\varepsilon^2(\text{eV})}, \quad (6a)$$

$$\tau_{e\text{-ph}}=\frac{1}{7\pi\zeta(3)\beta}\frac{h}{e}\frac{(P_F u_l)^2}{(\hbar\omega)^3}\ . \quad (6b)$$

These equations are valid for $\sim 10k\Theta_D > \varepsilon > kT$ and $\hbar\omega > kT$. The constants (h/e), β, and $\xi(3)$ are, respectively, equal to 4.2×10^{-15}, 0.5, and 1.2. The other variables in Eqs. 6(a) and 6(b) are: p_F, which represents the momentum at the Fermi surface; q_D, which represents the Debye phonon's momentum; u_l, which represent the longitudinal phonon velocity; and κ, is the Thomas Fermi screening momentum. For high-T_c materials we estimate $\kappa\approx p_F$, and $p_F u_l \approx k\Theta_D$. For Y-Ba-Cu-O the values for E_F (Ref. 21), Θ_D (Ref. 16), and u_l (Ref. 22) are, respectively, 0.25 eV, 371 K, and 5×10^3 m/sec. Substituting these values into Eqs. 6(a) and 6(b) we obtain Eqs. 7(a) and 7(b), respectively:

$$\tau_{ee}=\frac{2\times10^{-17}}{\varepsilon^2(\text{eV})}\ \text{sec}\ , \quad (7a)$$

$$\tau_{e\text{-ph}}=\frac{3.3\times10^{-19}}{(\hbar\omega)^3}\ \text{sec}\ . \quad (7b)$$

Initially, the electron's excess energy, $\varepsilon\approx2$ eV, is thermalized most efficiently by electron-electron interaction where half of the electron's excess energy is lost with each electron-electron interaction. With the electron-phonon interaction the energy each "hot" electron gives up is limited to the maximum energy of a phonon[23,24] ($\approx$50 meV). As each hot electron looses part of its excess energy, the electron-electron process slows down as $1/\varepsilon^2$ and the electron-phonon interaction becomes more likely. Estimation of when thermalization transition from cascading to phonon emission can be inferred from the relative values of τ_{ee} and $\tau_{e\text{-ph}}$ provided energy and momentum are conserved. The thermalization by the electron-phonon process occurs with the most energetic phonons ($\tau_{e\text{-ph}} \propto 1/\omega^3$) and with the largest electron-phonon coupling constant. Experimental indications[23,24] are that in Y-Ba-Cu-O the electron-phonon coupling constant is unusually strong, for the B_{1g} and A_g phonons as is evident from the line width of the Raman-active modes. The B_{1g} (out-of-phase oxygen plane vibration at 340 cm^{-1}) and the A_g (in-phase along Z of the oxygen plane vibration at 440 cm^{-1}) modes exhibit strong anharmonic linewidth broadening,[23] which is indicative of strong electron-phonon coupling. The $\tau_{e\text{-ph}}$ time constant based on the emission of an optical phonon ($Ep\approx50$ meV) is about 2.64×10^{-15} sec. The time constant τ_{ee}, for the interaction of 0.1-eV excess energy hot electrons [see Eq. 7(a)], is 2×10^{-15} sec. Thus it is expected that hot electrons, with about 0.1-eV excess energy, will transition from thermalization via an electron-electron process to an electron-phonon process. This transition energy is a rough estimate and is difficult to establish exactly. The electron-phonon thermalization process is expected to occur via emission of several optical phonons, in about 10^{-14} sec before the electrons reach the Fermi surface.

The emitted optical phonons decay into acoustic phonons within a time that can be estimated from the line width of the optical phonons.[25] The linewidths, at 90 K, of the optical-mode phonons,[23] strongly coupled with the electronic system, are 5 cm^{-1} (B_{1g}) and 8 cm^{-1} (A_g). These optical phonons quickly decay[23] into acoustical phonons in approximately 4 (A_g) and 7 psec (B_{1g}). As the temperature is increased from 90 to 200 K, the decay speeds up, due to anharmonic broadening, and occurs in about half the aforementioned times.[23] Thus after less than 10 psec the 2-eV photogenerated electrons will have transferred their energy into acoustical phonons resulting in TPR signals with a fast rise time. The TPR signal's rise time is slowed by the external trigger jitter ($\approx$15 psec), however, the data are consistent with the thermalization process described.

During the last stages of thermalization, phonons continue to interact with the electrons and gradually escape from the Y-Ba-Cu-O film into the substrate. An idealized model of this process, based on low-energy acoustic phonons, has been described by Little[26] and Anderson.[27] Using such a model Kaplan[28] provided a relationship for the escape rate τ_{es} in terms of the phonon's escape probability ζ, the phonon's velocity u_l, and the film thickness d, as

$$\tau_{es}=\frac{4D}{\zeta u_l}\ . \quad (8)$$

The acoustic transmission probability from Y-Ba-Cu-O into MgO (Ref. 29) (ζ) calculates to be about 0.5. For a 50-nm-thick Y-Ba-Cu-O film, the calculated escape time is 80 psec vs a measured relaxation time of 2.5 nsec (see Table II).

The discrepancy is attributed to a nonideal interfilm boundary[30] and the slower velocity[31–33] for the energetic phonons produced during thermalization,[22] as is evident from the Y-Ba-Cu-O phonon's dispersion spectrum.[32,33]

Recent experimental evidence[30] indicates that the interfilm thermal boundary is not ideal nor as expected from an acoustic model.[26–28] In fact the thermal resistance shows no temperature dependence and is 80 times larger than expected.[30] Thus the phonon escape probability ζ should be decreased from 0.5 to 0.0125. Using the smaller value of ζ, the τ_{es} calculates to 3.2 nsec vs 2.5 nsec for the measured value (see Table II). Accordingly the thermal model for the TPR signal above T_c is further supported.

B. Transition-state photoresponse

The transition-state TPR signal is examined in terms of photoresponse amplitude and signal decay time constant. The photoresponse amplitude, at T_c, is 30–60 times larger than the normal-state signal (see Table I) thereby making any kinetic inductance contributions negligible. Thus the sample at T_c is represented as a variable resistor $r(t)$; see Fig. 3. The combination of the dc bias current[34] and microscopic inhomogeneities broaden the transition temperature width to $\Delta T_c \leq 3$ K. Photoabsorption of the laser's fluence heats the films so as to decrease the fractional volume of the superconducting phase resulting in a TPR signal consistent with the bolometric response. Using Eq. (5) and the parameters in Table I, we calculated the photoresponse amplitude. The agreement obtained between measured and calculated values is typically within a factor of 2 with the worst case being within a factor of 3 (see Table IV). The discrepancies between measured and calculated photoresponse amplitude are attributed to measurements away from the transition temperature T_c and uncertainty in the adsorbed laser fluence. Deviation from the transition temperature T_c will decrease the photoresponse amplitude. The data for sample No. 3 (see Table IV) reveals that the film was not optimally at T_c, since its resistivity was 10 $\mu\Omega$ cm instead of $\rho(T_c)=35$ $\mu\Omega$ cm. Given that the sample's temperature was not optimal, the measured photoresponse, as expected, is less than the calculated value.

The TPR signal's relaxation time constant at T_c is larger than the time constant in the normal state (see Table II and Fig. 6). From the photoresponse amplitude it is evident that the photoresponse relaxation time at T_c corresponds to the time needed to increase the fraction of the superconducting phase volume as opposed to resistance changes in the normal regions. Recombination (τ_R) and reequilibrium near T_c is subject to and governed by the slower of two mechanisms: (1) the phonon escape rate from the sample into the substrate and (2) the relaxation of the order parameter (τ_Δ). Because of particle-hole symmetry[4] at T_c, the quasiparticle recombination lifetime (τ_R) equals the electron scattering lifetime (τ_S). Hence the observed photoresponse relaxation-time constant at T_c should equal the relaxation-time constants for the normal state. Thus the phonon bottle neck, observed for the normal state, imposes a lower limit on the TPR signal's relaxation-time constants at T_c. This lower limit for relaxation at T_c, established by Kaplan *et al.*,[4] does not include fluctuations in the Copper-pair field, which is important[35] within the Ginsburg-Landau critical region near T_c. Near T_c, the number of Cooper pairs is strongly dependent[36] on the order parameter Δ. Thus recombination of quasiparticles near T_c will be governed by the relaxation rate for the order parameter (τ_Δ), which diverges near T_c (Refs. 37–39 and 2) as

$$\tau_\Delta \propto \frac{\tau_S}{(1-T/T_c)^{1/2}} . \tag{9}$$

In view of Eq. (9) it is reasonable to conclude that at the transition temperature the relaxation-time constant will be larger than the relaxation-time constant in the normal state, and this is consistent with the data (see Fig. 6 and Table II).

TABLE IV. Transition state photoresponse of Y-Ba-Cu-O thin films.

Sample No.	T_c (K)	Responsivity $(1/\mu J)$ Measured	Calculated
1	86.8	0.76	0.71
2	85	0.43	0.32
3	85	0.308	0.69
4	87	1.12	0.86

C. Superconducting state photoresponse

The photoresponse in the superconductivity state is most complex because during the photoresponse the sample's state may temporarily change from a zero-resistance state into a resistive superconducting state.[15] Such a temporary transition from a zero-resistance superconducting state (inductive impedance) to a resistive superconducting state[11] complicates the time dependence of the photoinduced voltage transient. We start by examining the photoabsorption and thermalization process in the superconducting state. The information gleaned from this examination is used to calculate the photoresponse amplitudes. A comparison between the measured and calculated photoresponse amplitudes corroborates the claim that the photoresponse amplitude is due to changes in kinetic inductance. Finally, the time dependence of the photoresponse transients are examined.

Photoabsorption and thermalization in the superconducting state is similar to the photoabsorption process described in the normal state with some important differences. Initially, each photoabsorbed 2-eV photon will break a Cooper pair and form two quasiparticles, one with about 2 eV$-\Delta(T)$ of energy and the other with about $\Delta(T)$, where $\Delta(0)\approx 20$ meV (Ref. 22) at 0 K. Successive interaction between a hot quasiparticle and the Cooper-pair condensate continues to divide the excess energy by forming three quasiparticles. For example, a 2 eV$-\Delta$ quasiparticle will break a Cooper-pair producing three quasiparticles, two with about 1 eV$-\Delta$ of energy each and a third quasiparticle with about Δ of energy. The hot quasiparticles continue to break additional pairs by the electron-electron interaction process as they thermalize toward the energy gap by discrete energy

steps: 1 eV$-\Delta$ to 0.5 eV$-\Delta$ to 0.25 eV$-\Delta$ to 0.125 eV$-\Delta$. The interaction times, τ_{ee} and $\tau_{e\text{-ph}}$, for energetic quasiparticles, with energies several times (3–5) the gap energy, are the same as those for normal electrons. Using Eqs. 7(a) and 7(b) as before we estimate that quasiparticle thermalization transitions at about 0.1 eV from electron-electron interactions to an electron-phonon interactions. Thus after about four cascading interactions [$\varepsilon \approx 0.1$ eV≈ 0.125 eV$-\Delta(T)$] thermalizing quasiparticles will start emitting $\approx$40–50-meV phonons.[22–24] It is not possible to assign a single energy level where thermalization transitions from electron-electron to an electron-phonon process. However, we can claim that, on the average, each photoabsorbed 2-eV photon will break about 16 Cooper pairs by electron-electron interaction and emit about 32 ($\approx$50 meV) optical phonons. Thus the number of energetic phonons emitted during the last stage of thermalization is greater than the number of Cooper pairs broken by cascading. These energetic phonons will break, at a slower rate, additional Cooper pairs thereby increasing the quasiparticle population significantly beyond the number formed by cascading (see Fig. 8).

Although both the electron-electron and electron-phonon thermalization processes are very fast, in the superconducting state they have a different effect on the output signal. Cooper-pair breaking by electron-electron interaction is a direct process and shows up as an output signal because the TPR measurements are directly sensitive to the number of Cooper pairs broken. However, phonon emission, also very fast, does not produce an immediate output signal unless a net change occurs in the Cooper-pair populations. In fact, this excess phonon population will affect the Cooper-pair density significantly beyond the time wherein the phonons were emitted. The effective phonon pair breaking time is slower than cascading and depends on the number of Cooper pairs remaining,[4] the quasiparticle recombination rate, the excess phonon density, and the phonon escape rate from the film into the substrate.[27,28] The interplay between these different processes results in an extrinsic pair-breaking time by phonons, which is different and longer than the intrinsic time. A graphical description of the thermalization process is given in Fig. 8.

The thermalization process described produces nonequilibrium quasiparticle and phonon distributions, which cannot be described by an effective temperature or chemical potential. Clearly this experimental situation is different from theoretical models, which model a steady-state nonequilibrium state as an excess of quasiparticles[40] (μ^* model) or phonons[41] (T^* model). Under the transient nonequilibrium conditions described, the nonmonotonic quasiparticle population increases before finally decreasing (see Fig. 8), since the excess phonons break additional pairs before escaping slowly, as evident from the normal-state photoresponse decay time, into the substrate.

The measured and calculated values of the photoresponse amplitude are compared next. The photoresponse amplitude corresponds to and is produced by sudden changes in the sample's kinetic inductance occurring when quasiparticles are suddenly generated by electron-electron interaction (see Fig. 8 for times between t_0 and t_1). By evaluating Eq. (1) for very short times ($t < 10^{-14}$ sec) the output signal $e_{\text{osc}}(0_+)$ is related to changes in the kinetic inductance $\Delta\eta$ as

$$\Delta\eta = \frac{e_{\text{osc}}(0_+)}{I_0}\left[\frac{L_G}{50}\right] . \tag{10}$$

The relationship between $\Delta\eta$ and $e_{\text{osc}}(0_+)$ is valid even though it was obtained for times (10^{-14} sec) much shorter than the experimental setup is capable of resolving (70-GHz bandwidth reduced by $\sim$15 psec trigger jitter). Typically the photoresponse signal has a fast rise time and a much slower decay time (>100 psec). Thus the slower decay time makes it possible to measure the photoresponse amplitude,[11] albeit with a slower rise time ($\sim$30 psec). The measured photoresponse amplitude, $\mathcal{R}_M(T)$ (tabulated in Table II) has been normalized by the value of the initial kinetic inductance L^0_{KI} and the lasers fluence $L(\mu J)$, as follows:

$$\mathcal{R}_M(T) = \frac{\Delta\eta}{L^0_{\text{KI}} L(\mu J)} . \tag{11}$$

The calculated photoresponse amplitude, $\mathcal{R}_C(T)$, is based on changes in the kinetic inductance, $\eta(t)$, which are inversely proportional to the temperature-dependent Cooper-pair volume density[8,11,14] $n(T)$ and a geometrical constant A as

$$\eta(T) = \frac{A}{n(T)} . \tag{12}$$

A change in the sample's kinetic inductance $\Delta\eta$ is produced when an initial pair density $n_0(T)$ is reduced by cascading to an $n_1(T)$ pair density,

$$\Delta\eta = \frac{A}{n_1(T)} - \frac{A}{n_0(T)} . \tag{13}$$

Normalizing this expression according to Eq. (11) an expression for the and calculated responses $\mathcal{R}_C(T)$ is obtained:

$$\mathcal{R}_C(T) = \frac{n_0(T)-n_1(T)}{n_1(T)n_0(T)}\frac{n_i}{L(\mu J)} = \left[\left[\frac{L(\mu J)n_i(1-t^4)}{n_0(T)-n_1(T)} - L(\mu J)\right](1-t^4)\right]^{-1} , \tag{14}$$

where n_i is to the Cooper-pair density at 4.2 K (about[42,43] 7×10^{20} pairs/cm^3) and "t" is the reduced temperature defined as $t = T/(T_c + \Delta T_C)$ (see Table I). The number of broken pairs, $\Delta n = n_0(T) - n_1(T)$, broken during the cascading process, normalized by the laser's fluence $L(\mu J)$ is

$$\frac{\Delta n\,(\text{cm}^{-3})}{L(\mu\text{J})} = 16\frac{10^{-6}[1-\exp(-\alpha d)]T_{\text{op}}}{A_L d\,(3.2\times10^{-19}\ \text{J/photon})} , \tag{15}$$

where the leading coefficient, 16, corresponds to the estimated average number of Cooper pairs broken by cascading and the other terms have been introduced in Eq. (4). Combining Eqs. (14) and (15) the computed $\mathcal{R}_C(T)$

TABLE V. Photoresponse amplitude in Y-Ba-Cu-O in superconducting state using 7×10^{20} pairs/cm^2 (for sample Nos. 1, 2, and 3). As the maximum pair density value and London's two-fluid model. The temperatures used for the measured and calculated photoresponse are indicated in brackets. For sample No. 4, we used 3.5×10^{20} as the maximum pairs/cm^3 corresponding to the higher resistivity.

Sample No.	Broken pairs/cm^3 μJ	Measured and calculated normalized photoresponse R_C & R_M			
		Measured	Calculated	Measured	Calculated
4	8×10^{19}	0.37 (7 K)	0.30 (7 K)	0.39 (83 K)	5.07 (80 K)
1	8.7×10^{19}	0.11 (10 K)	0.14 (10 K)	2.32 (80 K)	1.69 (80 K)
2	5.8×10^{19}	0.08 (10 K)	0.09 (10 K)	0.06 (75 K)	0.45 (75 K)
3	7×10^{19}	0.19 (60 K)	0.19 (60 K)	1.13 (80 K)	2.2 (80 K)

and measured $\mathcal{R}_M(T)$ photoresponses were compared, and the results are listed in Table V.

The photoresponse is grouped into a region above and below 60 K (see Table V). Up to 60 K the photoresponse is weakly temperature dependent, and at about 60 K it begins to exhibit a strong temperature dependence as does[44] $n(T)$. Reasonable agreement between calculated and measured values is obtained for film Nos. 1, 2, and 3 (see Table V) up to 60 K. Sample No. 4 exhibits a higher measured response than the calculated value by about six times. A possible explanation for this difference is the film's higher than average resistivity (see Table I). It can be argued that the higher resistivity indicates a smaller normal carrier and Cooper-pair densities. If we estimate that for sample No. 4 the Cooper-pair density is only 50% (i.e., $n_i=3.5\times10^{20}$), improved agreement is obtained between the renormalized measured (0.37) and recalculated photoresponse (0.30) values.

Above 60 K, the photoresponse is larger and more temperature dependent, corresponding to the larger temperature dependence[44] of Cooper-pair density closer to T_c. The measured and calculated photoresponse values are typically larger at higher temperatures (see data in Table V). The agreement between measured and calculated values, although not as good as in the lower temperature region is qualitatively reasonable given the sensitivity of these calculated values of the Cooper-pair density. Also the temperature dependence of the average number (≈16) of pairs broken per photon by cascading was neglected. It is expected that as the temperature increases the number of pairs broken by electron cascading decreases, since there are fewer Cooper pairs. Thus closer to T_c the calculated values should give a poorer estimate of the measured photoresponse.

The small photoresponse measured at higher temperatures for sample No. 2 is unusual. The photoresponse of sample No. 2 is consistent with the other samples except at about 80 K. We attribute the discrepancy to poor focus of the laser beam during data taking at 80 K.

In the zero resistance state, the photoresponse amplitude is consistent with a quantum response as evident from its temperature dependence. A quantum response, inversely dependent on the Cooper-pair density, is expected to exhibit a strong temperature dependence[36,44] only close to T_c, and this is in agreement with the measured photoresponse, which is constant up to ≈60 K (see Fig. 10) and only increases closer to T_c (see Table V). If the observed photoresponse was thermal it would follow the temperature dependence T^3 of the specific heat.[16] The specific heat of the sample increases with temperature, so a thermal response, except at T_c, would be expected to decrease in amplitude with temperature [see Eqs. (4) and (5)]. The assertions of a quantum photoresponse are also supported by the observed "sign" and time dependence of the photoresponse described next.

In the zero-resistance superconducting state, the TPR signal's sign and temporal dependence are principally a manifestation of the time change in the sample's kinetic inductance[8,11] [see Fig. 3(b)]. The ac signal generated, $S(t)$, is dependent on the dc bias current, I_0, and the time derivative[45,46] of the kinetic inductance,[8,11]

$$S(t)\approx I_0\frac{d\eta}{dt}\approx-\frac{I_0}{[n(t)]^2}\frac{dn}{dt}\ , \tag{16}$$

where $n(t)$ is the temporal dependence of the Cooper-pair density.

The negative sign preceding the Cooper-pair density's time derivative, in Eq. (16), has important significance. Specifically, if the number of Cooper pairs is decreasing with time (quasiparticle generation) the output signal is positive. Correspondingly if the number of Cooper pairs is increasing with time (quasiparticle recombination) the output signal is negative. Moreover, the amplitude of the photoinduced transient will be more positive (negative) for a higher *rate* of generation (recombination) of quasiparticles. Hence a complete impedance transient record in the zero-resistance superconducting state should start from zero and become positive (quasiparticle generation) followed by a negative TPR signal (quasiparticle recombination) and back to zero as thermal equilibrium is reestablished[11] (see Fig. 8).

The leading edge of the photogenerated TPR signal is due to the rapid breaking of a Cooper pair caused by electron-electron interaction (cascading). The TPR signal remains positive, following the initial sharp rise, indicating (see Fig. 8) that pair breaking continues, but at a slower rate (smaller positive signal). Energetic phonons, emitted during the last phase of quasiparticle thermalization, continue to break additional pairs at a slower rate and are responsible for this positive signal portion. As the number of Cooper pairs is depleted, the pair-breaking rate decreases[4] and the TPR signal goes to zero. After a sufficient number of phonons escape into the substrate,

quasiparticle recombination begins producing a negative signal.

For the BCS-type superconductor the intrinsic pair-breaking time by phonons (τ_B) is computed by Kaplan *et al.*,[4] in units of τ_0^{ph}. The value of τ_0^{ph} is expressed in terms of the ion density of states (N ions/cm^3), the electron density of states [$N_E(E_F)$ states/eV cm^3], the energy gap at absolute zero [$\Delta(0)$ eV], and the squared electron-phonon interaction matrix element ($\langle\alpha^2\rangle_{av}$ eV) as

$$\tau_0^{ph}=\frac{N}{4\pi^2 N_E(E_F)\Delta(0)\langle\alpha^2\rangle_{av}} . \tag{17}$$

Substituting values in Eq. (17) for the ion density[47] ($N=7.5\times10^{22}$ ions/cm^3), the electron density of states[16,8] [$N_E(E_F)=4.5\times10^{22}$ states/eV cm^3], the energy gap parameter[22] [$\Delta(0)=21$ meV], and the squared electron-phonon interaction matrix element[48] ($\langle\alpha^2\rangle_{av}\cong22$ meV), we obtain $\tau_0^{ph}=0.057$ psec. Kaplan's computed value for τ_B at low temperature is comparable[4] to τ_0^{ph}. Clearly the measured extrinsic value of 150–300 psec (see Table II, Fig. 6) for τ_B on Y-Ba-Cu-O is much longer.

The discrepancy between experiment and calculations can be attributed to two reasons. First Y-Ba-Cu-O need not be a BCS-type superconductor; hence agreement with the calculations of Kaplan *et al.*[4] need not occur. A second explanation is that the experimental results are not measurements of the intrinsic quasiparticle generation or recombination lifetimes. In fact, the measured lifetimes critically depend on the phonon escape rate into the substrate subject to the boundary between the superconducting film and the substrate. Rothwarf and Taylor[49] have expressed this dependence with two equations written in terms of the excess quasiparticle Q and phonon P population as

$$\frac{d}{dt}\left[P+\frac{Q}{2}\right]=-\frac{P}{\tau_\gamma} , \tag{18a}$$

$$\frac{dQ}{dt}=\frac{P}{\tau_B}-\frac{(Q^2+2QQ_0)}{\tau_R} . \tag{18b}$$

Equation (18) is dependent on several parameters, which are the intrinsic quasiparticle recombination lifetime τ_R, the intrinsic pair-breaking time by a phonon τ_B, the effective time for depletion of pair-breaking phonons by an anharmonic phonon decay or escape into the substrate τ_γ, and the thermal equilibrium quasiparticle density Q_0. It is evident from Eqs. 18(a) and 18(b) that the quasiparticle generation or recombination rates are not intrinsic. What is measured are the net effective quasiparticle generation or recombination rates. For agreement to occur between calculated [see Eq. (17)] and measured (see Table II) values, the calculated τ_B value would have to increase by ≈1000 times. Such a large increase due to phonon trapping is unreasonable, and the discrepancy between calculated and measured τ_B is attributed to limitation in the theoretical model.[4].

It should be noted that the present results are in qualitative agreement with Kaplan *et al.*[4] predictions. An increase in the phonon pair-breaking time (τ_B) with temperature is predicted[4] and is experimentally observed on Y-Ba-Cu-O, where the decay time τ_B increases with temperature from ≈150 to ≈1000 psec (see Table II). The pair-breaking time τ_B increases, since, as the temperature increases, there are less pairs available to break and because of the phonon bottle neck.[49]

After a sufficient number of excess phonons escape into the substrate, recombination begins to dominate producing a negative (quasiparticle recombination) signal illustrated in Fig. 8. Long recombination-time constants are difficult to measure because all measurements were made by ac coupling the TPR signal to the oscilloscope[11] (see Figs. 2 and 3). Determination of the relaxation slope is limited by the 100-MHz low-frequency ac coupling-time constant (~15 nsec) of the bias T. However a negative TPR signal has been observed on a limited number of traces with a quasiparticle recombination time constant typically greater than 5 nsec.

The validity of the negative amplitude photoresponse signal is reinforced from measurements wherein the samples change states (see Fig. 9). The transient photoresponse signal in Fig. 9 starts with quasiparticle generation by electron cascading (steep rise up to point A in Fig. 9) followed by a reduced phonon-based pair-breaking rate, for approximately 160 psec, manifested as a reduced amplitude, until the local minimum (point B, Fig. 9). Next the photoresponse amplitude starts increasing for about 1.4 nsec until point C, and then it begins to decrease again. The local minimum (point B, Fig. 9) indicates a change from the zero-resistance superconducting state to the resistive[34] superconducting state occurring when the sample's dc bias current exceeds the sample's critical current. Pair breaking, in a resistive state, causes an increase in the samples resistance resulting in the photoresponse amplitude increasing. As the depairing rate decreases with time (point B to point C, Fig. 9), the increases in the photoresponse amplitude become more gradual until net recombination begins to occur at point C.

With net pair recombination starting (point C, Fig. 9), the resistance of the sample will start to decrease as is illustrated in Fig. 9. After a sufficient number of pairs recombine, the sample's critical current capacity will again exceed the value of the dc bias current. When this occurs, the sample will transition from the resistive state to the zero-resistance superconducting state, and a negative TPR signal amplitude is observed starting at point D in Fig. 9. Recombination continues beyond 10 nsec, where the limits of our instrument prevent us from measuring.

It should be noted that the location of point B, indicating a state change, should be sensitive to the bias current flowing through the sample. Biasing the sample with more current causes the transition to a resistive state to occur earlier, and this was observed in sample No. 3.

The change in the state (illustrated in Fig. 9) provides direct evidence that pair-breaking continues for a long time beyond the initial electron cascading process occurring in less than 10^{-13} sec. A local minimum in the photoresponse (see point B, Fig. 9) indicates that the sample is in a zero resistance state before and a resistive state

after. The time period between point A and C directly indicates that pair-breaking can occur for much longer times than expected from only an electron-electron thermalization process. Phonons, emitted during the last step of the initial thermalization process are responsible for continuing to break Cooper pairs for times significantly beyond what is expected from electron-electron interaction. It should be noted that the nonmonotonic response (i.e., local minimum at B, Fig. 9) does not occur when the sample is measured above T_c. This further corroborates the conclusion that the nonmonotonic response is associated with a state change.

V. SUMMARY

The photoresponse in Y-Ba-Cu-O was measured with a technique based on a transient photoimpedance response.[11] The photoresponse time dependence is strongly controlled by phonon dynamics described by the Rothwarf and Taylor equations.[49] Above and at T_c the photoresponse amplitude is consistent with a bolometric photoresponse. The photoresponse rise time is fast (<50 psec) and is limited by the measuring equipment. Examination of the photoabsorption process in Y-Ba-Cu-O for 2-eV photons indicates that electron-electron interaction dominates during the first phase of thermalization ($<10^{-13}$ sec). Transition to the emission of energetic phonons occurs for photoexcited electrons with about 0.1-eV excess energy. In the normal and transition states the fast thermalization gives rise to the observed fast signal rise times followed by a much slower signal decay attributed to the phonon bottle neck formed at the interface between the film and the substrate.

In the superconducting state the photoresponse is much more complex. Thermalization of the photoabsorbed 2-eV phonons occurs first by electron-electron interaction process that directly breaks Cooper pairs. It is estimated that the average number of pairs broken per each 2-eV photon is about 16. As in the normal and transition states, at about 0.1 eV the hot quasiparticles continue to decay by emission of energetic optical phonons. These energetic optical phonons decay into acoustical phonons (<10 psec) and continue to break additional Cooper pairs for a time period much longer than the initial cascading process.

In the superconducting state the photoresponse amplitude is proportional to the rate of change of the Cooper-pair density. Generation of Cooper pairs produces a positive signal, and recombination produces a negative signal. The leading edge of the photoresponse and its amplitude corresponds to the change in the sample's kinetic inductance caused by electron cascading. The positive decay portion of the photoresponse signal corresponds to additional pair breaking by phonons emitted during the last phase of the hot electrons thermalization process. Recombination of quasiparticles produces a negative signal.

With sufficient pair breaking, the sample may temporarily undergo a change from a zero-resistance superconducting state to a resistive superconducting state. This occurs when pair breaking diminishes the sample's critical current capacity below the dc bias current used in the measurements. Such a state change exhibits a nonmonotonic photoresponse manifesting the dependence of the output signal on the samples impedance. In the zero-resistance state the output is proportional to the time derivative of the kinetic inductance ($\propto 1/n$), while in the resistive state below T_c it is directly proportional to the pair density n. The nonmonotonic photoresponse give clear evidence that quasiparticle generation occurs for a long period of time (300 psec to 2 nsec). After sufficient recombination the samples return to the zero-resistance state as evident from a negative photoresponse signal.

The extrinsic nature of the quasiparticle generation and recombination rates, which are governed by phonon trapping in the film, has significant practical implications. Specifically, in principle, the acoustic characteristics of the interface and substrate could be engineered to adjust the nonequilibrium phonon lifetimes. Thus, in principle, the lifetime of quasiparticle recombination can be engineered to be much longer than the intrinsic lifetime value. Superconductors with quasiparticle lifetimes significantly longer than the intrinsic lifetime will make superconducting quantum detectors practical. Similarly, fast electronic devices can also be engineered by reducing phonon trapping effects in thin superconducting films.

ACKNOWLEDGMENTS

We thank D. K. Fork and M. Johnson for participating in some of these measurements. Some of the films were provided by C. B. Eom and D. K. Fork. Bill Oldfield contributed generously and critically to solving difficult hardware problems. Ted Geballe and Malcom Beasley were always very helpful and provided advice during the experimental phase of this program at Stanford and were instrumental in arranging the author's stay at Stanford. Michael Reizer generously shared his expertise in nonequilibrium superconductivity by answering many questions. This experiment would have been impossible without the laser provided by M. D. Fayer and operated by S. R. Greenfield and J. J. Stankus under Science Foundation Divisions of Materials Research support Contract No. DMR87-18959 and ONR Contract No. N00014-89-J-1119. Dr. G. Strull arranged at Westinghouse the financial support, which made this project possible. Finally, John Talvacchio and Martin Forrester provided Y-Ba-Cu-O films and gave valuable information and advice. This work was supported in part by AFOSR Contract No. F49620-88-K-002, and Westinghouse independent research and development funds under task No. Z60601EHZB1.

[1]Jhy-Jium Chang, in *Non-Equilibrium Superconductivity, Phonons, and Kapitza Boundaries,* edited by Kenneth E. Gray (Plenum, New York, 1980), p. 263.
[2]A. M. Kadin and A. M. Goldman, in *Non-Equilibrium Superconductivity,* Vol. 12 of *Modern Problems in Condensed Matter Sciences,* edited by V. M. Agranovich and A. A. Maradudin (Elsevier Science, Amsterdam, 1986), p. 253.
[3]D. N. Langenberg, *Proceedings of the 14th International Conference on Low Temperature Physics, Ontamiemi, Finland, 1976,* edited by M. Krusius and M. Vuorio (North-Holland, Amsterdam, 1975), Vol. 5, p. 223.
[4]S. B. Kaplan, C. C. Chi, D. N. Langenberg, J. J. Chang, S. Jafarey, and D. J. Scalapino, Phys. Rev. B **14**, 4854 (1976).
[5]Barry I. Miller and Aly. H. Dayem, Phys. Rev. Lett. **18**, 1000 (1967).
[6]M. Tinkham and J. Clark, Phys. Rev. Lett. **28**, 1366 (1972).
[7]G. J. Dolan and L. D. Jackel, Phys. Rev. Lett. **39**, 1628 (1977).
[8]T. Van Duzer and C. W. Turner, *Principles of Superconductive Devices and Circuits* (Elsevier, New York, 1981), p. 114.
[9]R. Peters and H. Meissner, Phys. Rev. Lett. **30**, 965 (1973).
[10]L. R. Testardi, Phys. Rev. B **4**, 2189 (1971).
[11]N. Bluzer (unpublished).
[12]J. I. Gittleman, B. Rosenblum, T. E. Seidel, and A. W. Wicklund, Phys. Rev. **137**, A527 (1965); J. I. Gittleman and B. Rosenblum, Proc. IEEE **52**, 1138 (1964).
[13]Albert Schmid, Phys. Rev. **196**, 420 (1969).
[14]F. London, *Superfluids* (Wiley, New York, 1950), Vol. 1.
[15]N. Bluzer, D. K. Fork, T. H. Geballe, M. R. Beasley, M. R. Reizer, S. R. Greenfield, J. J. Stankus, and M. Fayer, Proceedings of the 1990 Applied Superconductivity Conference, Snow Mass, Colorado 1990 [IEEE Trans. Magn. **MAG-27**, 1519 (1991)].
[16]H. E. Fisher, S. K. Watson, and D. G. Cahill, Comments Mod. Phys. B **14(2)**, 65 (1988).
[17]I. Bozovic, Phys. Rev. B **42**, 1969 (1990).
[18]A. A. Abrikosov, L. P. Gorkov, and I. E. Dzyaloshinski, *Methods of Quantum Field Theory in Statistical Physics* (Prentice-Hall, Englewood Cliffs, NJ, 1963).
[19]M. Y. Reizer, Phys. Rev. B **39**, 1602 (1989); **40**, 5411 (1989).
[20]The expressions for $\kappa = u\pi e^2 \nu$ and $\beta - 2\varepsilon_F \nu / 3MNu_l^2$ are taken from Ref. 19. For a free-electron gas we approximate $\kappa \approx P_F$ and $\beta \approx 0.5$. The variables used to compute κ and β are: ν the electronic two-spin density of states; M the ionic mass per unit cell; N the density of unit cells, and u_l the acoustic velocity.
[21]V. Z. Kresin, G. Deutcher, and S. A. Wolf, Supercond. **1**, 327 (1988).
[22]P. Baumgart, S. Blumenroder, A. Erle, B. Hillenbrands, P. Splittgerber, G. Guntherodt, and H. Schmidt, Physica C **162-164**, 1073 (1989).
[23]B. Friedl, C. Thomsen, and M. Cardona, Phys. Rev. Lett. **65**, 915 (1990).
[24]R. E. Cohen, W. E. Pickett, and H. Krakauer, Phys. Rev. Lett. **64**, 2575 (1990); R. E. Cohen, W. E. Pickett, and H. Krakauer, Phys. Rev. Lett. **62**, 831 (1989).
[25]M. Y. Reizer, Phys. Rev. B **38**, 10 398 (1988).
[26]W. A. Little, Can. J. Phys. **37**, 334 (1959).
[27]A. C. Anderson, in *Non-Equilibrium Superconductivity, Phonons, and Kapitza Boundaries* (Ref. 1).
[28]S. B. Kaplan, J. Low Temp. Phys. **37**, 343 (1979).
[29]*Handbook of Laser Science and Technology,* edited by M. Weber (CRC, Boca Raton, 1987), Vol. IV.
[30]M. Nahum, S. Verghese, P. L. Richard, and K. Char (unpublished).
[31]C. Kittel, *Introduction to Solid State Physics,* 3rd ed. (Wiley, New York, 1968), p. 146.
[32]W. Reichardt, D. Ewert, E. Gering, F. Compf, L. Pintschovius, B. Renker, G. Collin, A. J. Dianox, and H. Mutka, Physica B **156-157**, 897 (1989).
[33]W. Reichardt, L. Pintschovius, B. Hennion, and F. Collins, Supercond. Sci. Technol. **1**, 173 (1988).
[34]M. Tinkham, *Introduction to Superconductivity* (Krieger, Malabar, 1985), pp. 99 and 168.
[35]M. Cyrot, Rep. Prog. Phys. **36**, 103 (1973).
[36]J. R. Schrieffer, *Theory of Superconductivity* (Addison-Wesley, Reading, MA, 1964), p. 54.
[37]A. Schmid and G. Shon, J. Low Tem. Phys. **20**, 107 (1975).
[38]I. Schuller and K. E. Gray, Phys. Rev. Lett. **36**, 429 (1976).
[39]I. Schuller and K. E. Gray, Solid State Commun. **23**, 337 (1977).
[40]C. S. Owen and D. J. Scalapino, Phys. Rev. Lett. **28**, 1559 (1972).
[41]W. H. Parker, Phys. Rev. B **12**, 3667 (1975).
[42]B. Pümpin, H. Keller, W. Kundig, W. Odermatt, I. M. Savić, J. W. Schneider, H.Simmler, P. Zimmermann, J. G. Bednorz, Y. Maeno, R. A. Müller, C. Rossel, E. Kaldis, S. Rusiecki, W. Assmus, and J. Kowalewski, Physica C **162-144**, 151 (1989).
[43]The density of Cooper pairs was calculated from the measured penetration depth (1400 Å) given by Ref. 38 and the expression relating the London penetration depth in terms of the Cooper-pair density; see Refs. 8 and 11.
[44]M. Tinkham, *Introduction to Superconducitivity* (Ref. 34), p. 80; the temperature dependence of the Cooper-pair density is taken to be proportional to $1-t^4$, where t is the reduced temperature.
[45]R. P. Feynman, R. B. Leighton, and M. Sands, *The Feynman's Lectures on Physics* (Addison-Wesley, Reading, MA, 1964), pp. 22-4 and 22-5.
[46]W. H. Hayt, Jr. and J. E. Kemmerly, *Engineering Circuits Analysis* (McGraw-Hill, New York, 1962), p. 106.
[47]A. Junod, A. Bezinge, D. Cattani, M. Decroux, D. Eckert, M. Francois, A. Hewat, J. Muller, and K. Yvon, Helv. Phys. Acta **61**, 460 (1988).
[48]Philip B. Allen (private communication), and using the definition for γ [see W. L. McMillan, Phys. Rev. **167**, 331 (1968)] combined with the estimate for $\lambda \cong 1-2$, the average phonon frequency energy of 3 meV combined with Kaplan's expression (Ref. 4) for $\langle \alpha^2 \rangle_{av}$.
[49]A. Rothwarf and B. N. Taylor, Phys. Rev. Lett. **19**, 27 (1967).